Supplementary Material for

Cross-interface model for the thermal transport across interface between overlapped nanoribbons

Wentao Feng[1,2], Xiaoxiang Yu[2], Yue Wang[2], Dengke Ma[2,3], Zhijia Sun[4], Chengcheng Deng[1,2]* and Nuo Yang[1,2]*

[1] State Key Laboratory of Coal Combustion, Huazhong University of Science and Technology, Wuhan 430074, P. R. China

[2] School of Energy and Power Engineering, Huazhong University of Science and Technology, Wuhan 430074, P. R. China

[3] NNU-SULI Thermal Energy Research Center (NSTER) & Center for Quantum Transport and Thermal Energy Science (CQTES), School of Physics and Technology, Nanjing Normal University, Nanjing 210023, P. R. China

[4] Institute of High Energy Physics, Chinese Academy of Sciences, Beijing 100049, China;

* Corresponding email: dengcc@hust.edu.cn (C.D.); nuo@hust.edu.cn (N.Y.)

1. MD simulation details

Non-equilibrium molecular dynamics (NEMD) simulation is performed to study the thermal transport at the cross-interface. The optimized Tersoff potential is applied to describe covalent bonding in BN nanoribbon. The interactions between BN nanoribbons are van der Waals forces modeled by the Lennard-Jones potential. The parameters for the potentials used in the work are shown in Table S1. Firstly, an energy minimization of the system is performed and the simulation box is also relaxed. Secondly, BN nanoribbons are relaxed in the canonical ensemble (NVT) and microcanonical ensemble (NVE) respectively for 0.25ns and 0.1ns at 300K. Then, the heat source and heat sink are applied. And the system are run for 2.5 ns to reach a steady state. The following 25ns is used to get the temperature and the heat flux in the system.

Table S1. MD simulation details and parameters [1].

Method	Non-Equilibrium Molecular Dynamics (Direct method)
Potential (TERSOFF/Lennard-Jones)	
Function (TERSOFF)	$$E=\frac{1}{2}\sum_{i}\sum_{j(\neq i)}V_{ij}$$ $$V_{ij}=f_C(r_{ij})\left[f_R(r_{ij})+b_{ij}f_A(r_{ij})\right]$$ $$f_C(r_{ij})=\begin{cases}1, r_{ij}<R_{ij}\\ \frac{1}{2}+\frac{1}{2}\cos\left(\pi\frac{r_{ij}-R_{ij}}{S_{ij}-R_{ij}}\right), R_{ij}<r_{ij}<S_{ij}\\ 0, \quad r_{ij}>S_{ij}\end{cases}$$ $$f_R(r_{ij})=A_{ij}exp(-\lambda^{\mathrm{I}}_{ij\,1}r_{ij})$$ $$f_A(r_{ij})=-B^{'}_{ij}exp\left(-\lambda^{\mathrm{II}}_{ij}r_{ij}\right),\qquad B^{'}_{ij}=B_{ij}\chi_{ij}$$ $$b_{ij}=(1+\beta_i\varsigma_{ij}^{n_i})^{-\frac{1}{2n_i}},\quad \varsigma_{ij}=\sum_{k\neq i,j}f_C(r_{ik})g(\theta_{ijk})$$ $$g(\theta_{ijk})=(1+\frac{c_i^2}{d_i^2}-\frac{c_i^2}{\left[d_i^2+(cos\theta_{ijk}-h_i)^2\right]})$$

Parameters / Elements	m	χ	c	d	$cos\theta$	n	β	λ^{II}	B	R	S	λ^{I}	A
Units	***1***	***1***	***1***	***1***	***1***	***1***	***1***	***1/Å***	***eV***	***Å***	***Å***	***1/Å***	***eV***
NBB	3	1	25000	4.348	-0.89	0.728	1.257e-7	2.199	340	1.95	0.05	3.568	1380
NBN	3	1	25000	4.348	-0.89	0.728	1.257e-7	2.199	340	1.95	0.05	3.568	1380
BNB	3	1	25000	4.348	-0.89	0.728	1.257e-7	2.199	340	1.95	0.05	3.568	1380
BNN	3	1	25000	4.348	-0.89	0.728	1.257e-7	2.199	340	1.95	0.05	3.568	1380
NNB	3	1	17.796	5.948	0	0.618	0.0193	2.627	138.779	2	0.1	2.829	128.869
NNN	3	1	17.796	5.948	0	0.618	0.0193	2.627	138.779	2	0.1	2.829	128.869
BBB	3	1	0.526	0.00159	0.5	3.993	1.6e-6	2.077	43.132	2	0.1	2.237	40.052
BBN	3	1	0.526	0.00159	0.5	3.993	1.6e-6	2.077	43.132	2	0.1	2.237	40.052

Function (LJ)	$V_{ij} = 4\varepsilon\left[\left(\frac{\sigma}{r}\right)^{12} - \left(\frac{\sigma}{r}\right)^{6}\right]$

Parameters / Elements	σ(Å)	$\varepsilon\ (eV)$
NN	3.261	0.002992
NB	3.449	0.004833
BB	3.638	0.007806

Simulation process

Timestep	0.25fs			
Boundary Conditioon	X, Y, Z: free, free, periodic			
Ensemble	**Setting**			**Purpose**
NVT	Runtime (ns)	0.25ns		Relax Structure
	Temperature (K)	300		
NVE	Runtime (ns)	0.1ns		
	Temperature (K)	300		
NVE	Runtime (ns)	2.5ns		Reach Steady-State
	Thermostat	Heat source	320K	
		Heat sink	280K	
	Runtime (ns)	25ns		Record Information
	Thermostat	Heat source	320K	
		Heat sink	280K	

Recorded physical quantity

Temperature	$< E >= \sum_{i=1}^{N} \frac{1}{2} m v_i^2 = \frac{1}{2} N k_B T_{MD}$
Heat flux	$J = \frac{1}{N_t} \sum_{i=1}^{N_t} \frac{\Delta \varepsilon_i}{2\Delta t}$

Thermal conductivity	$\kappa = -\frac{J}{W \cdot d \cdot \nabla T}$

2. Adhesion energy

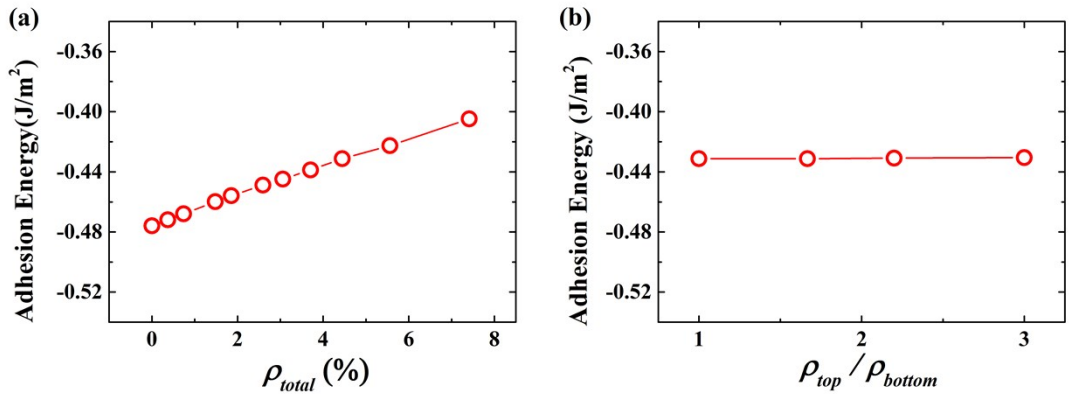

Figure S1 Adhesion energy calculated as a function of the (a) total vacancy concentration ρ_{total} and (b) vacancy concentration ratio between two nanoribbons ρ_{top}/ρ_{bottom}.

To explore the reasons for the increased interfacial thermal resistance (R_{inter}) with total vacancy concentration ρ_{total} and unchanged R_{inter} with vacancy ratio ρ_{top}/ρ_{bottom}, the adhesion energy between two BN nanoribbons is calculated. It has been investigated before that the reduced adhesion energy would lead to the increase of the interfacial thermal resistance [2-4]. And as shown in Fig. S1, adhesion energy decrease obviously with vacancy concentration while stay unchanged with vacancy ratio. Therefore, the reasons for the trend of R_{inter} with vacancy concentration and ratio is explained.

3. Structure of the boron nitride nanoribbons after relaxation

The structure of the system after relaxation is shown in Figure S2. There are still some observable fluctuations in the system, which is acceptable in MD simulations of two-dimensional system [5, 6]. But it is notable that fluctuations are not the bending that caused by the unrelaxed stress, because fluctuations only exist in the boundary as

shown in Figure S2(b). If the atoms at the boundary are removed in Figure S2(c, d), there are less fluctuations in the structure.

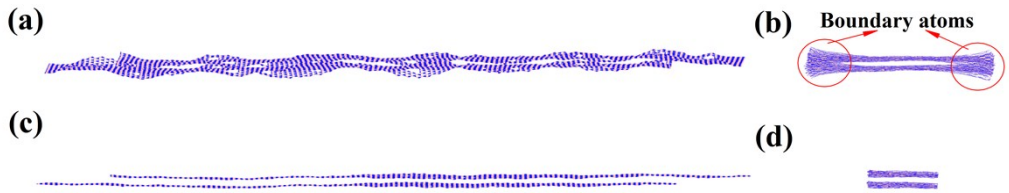

Figure S2. Schematic of the BN nanoribbon after relaxation in (a) front view and (b) side view. Schematic of the BN nanoribbon without boundary atoms after relaxation in (c) front view and (d) side view.

4. Comparison of thermal conductivity with literature

In order to verify the reliability of the simulation results, the values of thermal conductivity of pristine BNNRs are calculated and compared with the previous literature, as shown in Figure S3 [7]. The results are in good agreement with previous results, which shows that simulations are reliable.

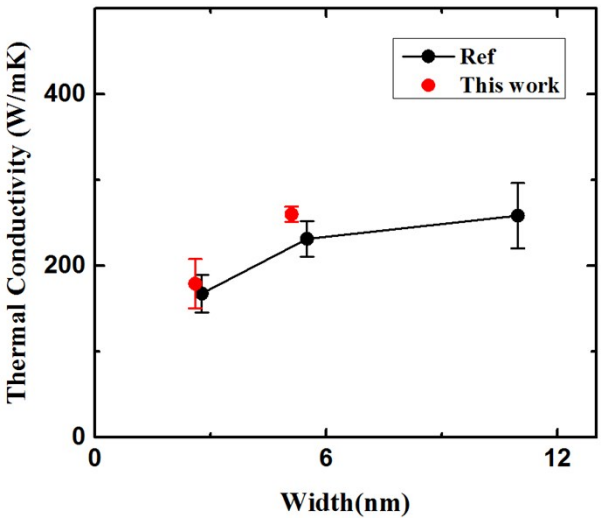

Figure S3. Comparing the thermal conductivity of pristine BNNR with the results in Ref. [7].

[1] A. Kınacı, J. B. Haskins, C. Sevik, and T. Çağın, Physical Review B **86** (2012).

[2] R. Prasher, Applied Physics Letters **94** (2009).

[3] F. Sun, T. Zhang, M. M. Jobbins, Z. Guo, X. Zhang, Z. Zheng, D. Tang, S. Ptasinska, and T. Luo, Adv Mater **26** 6093 (2014).

[4] H. Harikrishna, W. A. Ducker, and S. T. Huxtable, Applied Physics Letters **102** (2013).
[5] J. H. Zou and B. Y. Cao, Applied Physics Letters **110** 103106 (2017).
[6] MORTAZAVI, Bohayra, AHZI, and Saïd, Carbon **63** 460 (2013).
[7] C. Sevik, A. Kinaci, J. B. Haskins, and T. Çağın, Physical Review B **84** (2011).